

See discussions, stats, and author profiles for this publication at: <https://www.researchgate.net/publication/273325727>

Synthesis and in Vitro and in Vivo Evaluation of an 18 F-Labeled Neuropeptide Y Analogue for Imaging of Breast Cancer by PET

ARTICLE in MOLECULAR PHARMACEUTICS · MARCH 2015

Impact Factor: 4.38 · DOI: 10.1021/mp500601z · Source: PubMed

CITATION

1

READS

92

5 AUTHORS, INCLUDING:



[Sven Hofmann](#)

St George's, University of London

3 PUBLICATIONS 14 CITATIONS

[SEE PROFILE](#)



[Torsten Kuwert](#)

Friedrich-Alexander-University of Erlangen-...

285 PUBLICATIONS 5,114 CITATIONS

[SEE PROFILE](#)



[Annette G Beck-Sickinger](#)

University of Leipzig

356 PUBLICATIONS 9,723 CITATIONS

[SEE PROFILE](#)



[Olaf Prante](#)

Friedrich-Alexander-University of Erlangen-...

69 PUBLICATIONS 974 CITATIONS

[SEE PROFILE](#)

Synthesis and *in Vitro* and *in Vivo* Evaluation of an ¹⁸F-Labeled Neuropeptide Y Analogue for Imaging of Breast Cancer by PET

Sven Hofmann,[†] Simone Maschauer,[‡] Torsten Kuwert,[‡] Annette G. Beck-Sickinger,[†] and Olaf Prante^{*‡}

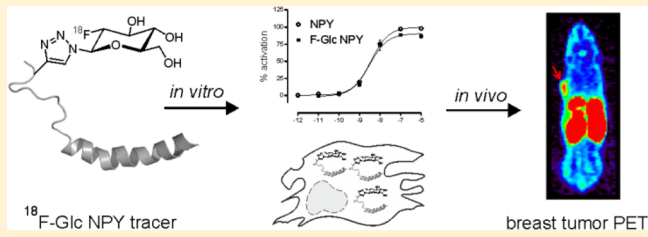
[†]Faculty of Biosciences, Pharmacy and Psychology, Institute of Biochemistry, Universität Leipzig, 04109 Leipzig, Germany

[‡]Department of Nuclear Medicine, Molecular Imaging and Radiochemistry, Friedrich-Alexander-Universität Erlangen-Nürnberg (FAU), 91054 Erlangen, Germany

Supporting Information

ABSTRACT: Imaging of Y₁R expression in breast cancer is still a challenging task. Herein, we report a suitable ¹⁸F-labeled high-molecular-weight glycopeptide for imaging of peripheral neuropeptide Y (NPY) Y₁ receptor (Y₁R)-positive tumors by preclinical small-animal positron emission tomography (PET). The Y₁R-preferring NPY [F⁷P³⁴]NPY analogue was functionalized with an alkyne-bearing propargylglycine (Pra) in position 4. The corresponding fluoroglycosylated (FGlc) peptide analogue [Pra⁴(FGlc),F⁷P³⁴]NPY and its ¹⁸F-labeled analogue were synthesized by click chemistry-based fluoroglycosylation. The radiosynthesis was performed by ¹⁸F-fluoroglycosylation starting from the 2-triflate of the β -mannosylazide and the alkyne peptide [Pra⁴,F⁷P³⁴]NPY. The radiosynthesis of the ¹⁸F-labeled analogue was optimized using a minimum amount of peptide precursor (40 nmol), proceeding with an overall radiochemical yield of 20–25% (nondecay corrected) in a total synthesis time of 75 min with specific activities of 40–70 GBq/ μ mol. In comparison to NPY and [F⁷P³⁴]NPY, *in vitro* Y₁R and Y₂R activation studies with the cold [Pra⁴(FGlc),F⁷P³⁴]NPY on stably transfected COS-7 cells displayed a high potency for the induction of Y₁R-specific inositol accumulation ($pEC_{50} = 8.5 \pm 0.1$), whereas the potency at Y₂R was significantly decreased. Internalization studies on stably transfected HEK293 cells confirmed a strong glycopeptide-mediated Y₁R internalization and a substantial Y₁R subtype selectivity over Y₂R. *In vitro* autoradiography with Y₁R-positive MCF-7 tumor tissue slices indicated high specific binding of the ¹⁸F-labeled glycopeptide, when binding was reduced by 95% ([Pra⁴,F⁷P³⁴]NPY) and by 86% (BIBP3226 Y₁R antagonist) in competition studies. Biodistribution and small-animal PET studies on MCF-7 breast tumor-bearing nude mice revealed radiotracer uptake in the MCF-7 tumor of 1.8%ID/g at 20 min p.i. and 0.7%ID/g at 120 min p.i. ($n = 3–4$), increasing tumor-to-blood ratios from 1.2 to 2.4, and a tumor retention of $76 \pm 4\%$ ($n = 4$; 45–90 min p.i.). PET imaging studies with MCF-7 tumor-bearing nude mice demonstrated uptake of the ¹⁸F-labeled glycopeptide in the tumor region at 60 min p.i., whereas only negligible tumor uptake was observed in animals injected with a nonbinding ¹⁸F-labeled glycopeptide pendant as a measure of nonspecific binding. In conclusion, PET imaging experiments with the ¹⁸F-labeled NPY glycopeptide revealed Y₁R-specific binding uptake in MCF-7 tumors *in vivo* together with decreased kidney uptake compared to DOTA-derivatives of this peptide. We consider this glycopeptide to be a potent lead peptide for the design of improved ¹⁸F-glycopeptides with shorter amino acid sequences that would further facilitate PET imaging studies of Y₁R-positive breast tumors.

KEYWORDS: fluorine-18, peptide, glycosylation, positron emission tomography, neuropeptide Y, NPY



INTRODUCTION

G-protein coupled receptors (GPCRs) emerged as highly attractive molecular targets for advanced drug screening, discovery, and development process.^{1,2} Among these, especially peptide hormone receptors play a crucial role in cancer research. They have been found to be overexpressed in various tumors, primary and or metastatic.³ Consequently, their high-affinity peptide ligands can be exploited as *in vivo* cargo shuttles.^{4,5} Thus, stabilized and multifunctionalized peptides provide a selective and controlled delivery system for diagnostic probes or therapeutic agents to cancerous tissue.⁶

In breast cancer, the human neuropeptide Y receptor (YR) system has been found to be of high pathophysiological relevance. Apart from other peptide hormone receptors such as

somatostatin, vasoactive intestinal peptide, and gastrin-releasing peptide receptors, the human Y₁ receptor subtype (Y₁R) has been found to be highly overexpressed in 85% of primary breast cancer and in 100% of lymph node metastases.^{7,8} Although the Y₁R is present in various epithelial, endocrine, and embryonal tumors, it has the highest incidents and density in breast cancer.⁹ The Y₁R is part of a multireceptor system comprising three further subtypes, namely, Y₂R, Y₄R, and Y₅R.¹⁰ Belonging to the rhodopsin-like GPCRs, they transduce extracellular

Received: September 7, 2014

Revised: January 24, 2015

Accepted: March 6, 2015

stimuli through inhibitory $G\alpha_{i/o}$ -proteins and subsequent receptor internalization.^{11–13} In contrast to Y₁R, the Y₂R subtype is primarily present in normal breast tissue and expression is rare and at low level in cancerous breast tissue.⁷ As proof of principle for specific imaging of primary and metastatic breast cancer by Y₁R targeting peptides, selective tumor uptake of a ^{99m}Tc-labeled Y₁R-preferring NPY analogue, [F⁷,P³⁴]NPY, has been demonstrated in breast cancer patients.¹⁴

The three endogenous ligands of the YR system, neuropeptide Y (NPY), pancreatic polypeptide (PP), and peptide YY (PYY), comprise the homologous neuropeptide Y family (NPY-family).^{15,16} While all are characterized by a tyrosine-rich 36 amino acid sequence and C-terminal amidation, NPY and PYY preferentially activate the Y₁R, Y₂R, and Y₅R,¹⁷ whereas PP primarily acts at the Y₄R.¹⁸ Extensive structure–activity relationship studies focusing on the multireceptor and multiligand site have provided the fundamental insights required for the design of YR subtype selective ligands.^{19,20} With respect to Y₁R preferring full-length analogues, [L³¹,P³⁴]NPY and [F⁷,P³⁴]NPY have successfully been developed.^{21,22} *In vivo* and *in vitro* studies with [F⁷,P³⁴]NPY have identified position 4 to be a suitable modification site for further functionalization.^{23,24} These modifications included the introduction of large hydrophobic carbaboranes as an approach toward targeted boron neutron capture therapy and the synthesis of the DOTA-linked analogue [K⁴(DOTA),F⁷,P³⁴]-NPY for subsequent radiolabeling with ¹¹¹In for SPECT imaging of Y₁R expression. *In vitro* and *in vivo* studies suggested promising characteristics; however, future applications in nuclear medicine for breast tumor diagnosis and therapy have not yet been reported.

Recently, the diaminopyridine derivative [¹⁸F]Y1–973 has been reported as the first nonpeptide PET tracer suitable for central Y₁R imaging in nonhuman primates.²⁵ [¹⁸F]Y1–973 revealed excellent properties for brain imaging of Y₁R expression; however, its high lipophilicity together with significant liver accumulation predicts that its peripheral application for breast cancer imaging is less suitable. Therefore, an appropriate ¹⁸F-labeled PET tracer for *in vivo* imaging of Y₁R expression in breast tumors is still needed.

On the basis of our previous work on the strategy for ¹⁸F-fluoroglycosylation of alkyne-bearing peptides using the click chemistry approach,^{26–28} we aimed at the development of a full-length NPY analogue bearing a glycosylation site in position 4 of the amino acid sequence. As the [F⁷,P³⁴]NPY analogue has already proven *in vivo* applicability,²³ we developed a suitable peptide precursor bearing the alkyne functionality in position 4, allowing regiospecific ¹⁸F-labeling by ¹⁸F-fluoroglycosylation using click chemistry. In this work, we studied the *in vitro* properties of the resulting NPY glycopeptide with respect to selective Y₁R targeting over Y₂R, including internalization and signal transduction assays, and characterized the biodistribution and specific binding of the ¹⁸F-labeled NPY glycopeptide *in vivo* by small-animal PET studies of MCF-7 breast tumor-bearing nude mice.

EXPERIMENTAL SECTION

Synthesis of Fluoroglycosylated NPY Analogues. The solid phase peptide syntheses are described in the Supporting Information. The alkyne functionalized NPY peptide (**3a** or **4a**) was dissolved in acetonitrile and diluted with 0.2 mM sodium phosphate buffer (pH 8) to 0.1 mM to a final acetonitrile

concentration of 20%. Freshly prepared CuSO₄ (stock solution 1.2 mM in H₂O) and 2-deoxy-2-fluoro- β -D-glucopyranosyl azide²⁷ (stock solution 50 mM) were added in equimolar stoichiometry under constant stirring and argon flow. The click reaction was initiated by adding three equivalents of ascorbic acid (stock solution 3.6 mM in H₂O). The reaction was completed within 30 min at 50 °C under constant stirring and argon flow. The fluoroglycosylated product (**3b** or **4b**) was isolated by semipreparative reversed phase high-performance liquid chromatography (RP-HPLC) applying an adapted two-step gradient elution system composed of 20 to 30% solvent B over 5 min (step 1) and 30 to 50% solvent B over 40 min (step 2). Corresponding fractions containing the correct mass and homogeneity >95% were pooled and reanalyzed by RP-HPLC and mass spectroscopy (MS) to verify both purity and identity (see Table S1).

Radiosynthesis of ¹⁸F-Fluoroglycosylated NPY Analogue [¹⁸F]3b and [¹⁸F]4b. Using the precursor 3,4,6-tri-O-acetyl-2-O-trifluoromethanesulfonyl- β -D-mannopyranosyl azide,²⁶ 2-deoxy-2-[¹⁸F]fluoroglucopyranosyl azide was synthesized as described previously.²⁷ The resulting solution (NaOH, 60 mM) was adjusted to pH 8 with HCl (0.1 M, 9 μL) and a solution of **3a** or **4a** (40 nmol in 80 μL ethanol), sodium ascorbate (100 mM, 10 μL), CuSO₄ (4 mM, 10 μL), and THPTA (tris(hydroxymethyl)triazolylmethyl)amine, 20 mM, 10 μL) were added, and the reaction mixture was stirred for 10 min at 50 °C. [¹⁸F]3b or [¹⁸F]4b was isolated by semi-preparative HPLC (PerfectSil 300 C4, 125 × 8 mm, 4 mL/min, 30–50% acetonitrile (0.1% TFA) in water (0.1% TFA) in a linear gradient over 20 min, *t*_R([¹⁸F]3b) = 8.5 min, *t*_R([¹⁸F]4b) = 9.5 min) and subsequent solid phase extraction (SPE, Lichrosorb, Merck, 100 mg). [¹⁸F]3b or [¹⁸F]4b (120–170 MBq) was eluted from the cartridge with 1 mL of ethanol/PBS (1:1 v/v), the solvent was evaporated in vacuo, and the radiopeptide was dissolved in PBS (pH 7.4) for *in vitro* and *in vivo* use. The ¹⁸F-labeled glycopeptides were identified by retention time (*t*_R) by means of the radio-HPLC system and by coinjection of the corresponding reference compound (Kromasil C8, 250 × 4.6 mm, 20–70% acetonitrile (0.1% TFA) in water (0.1% TFA) in a linear gradient over 30 min, 1.5 mL/min, *t*_R(3b) = 14.6 min, *t*_R(4b) = 15.7 min). [¹⁸F]3b (*n* = 7) or [¹⁸F]4b (*n* = 2) were obtained with specific activities of 40–70 GBq/μmol in overall radiochemical yields of 20–25% (not corrected for decay, referred to used [¹⁸F]fluoride) in a total synthesis time of 75 min.

In Vitro Characterization. Inositol Phosphate Accumulation Assay. Receptor activation after peptide ligand stimulation was investigated as previously described.²⁹ Briefly, stably transfected COS-7 cells expressing either the Y₁R or the Y₂R and a chimeric Gα_{Δ6q4myr}-protein³⁰ were used. Thus, the endogenous inhibitory Gα_i-pathway was switched to the Gα_q-pathway leading to inositol phosphate production after peptide ligand stimulation. Cells were seeded into 48-well plates and grown to 90% confluence. After radioactive labeling with [³H]myo-inositol (2 μCi/mL), cells were stimulated over 1 h with increasing concentrations of peptide ranging from 10 pM to 1.0 μM. Followed by basic cell lysis and subsequent neutralization, the supernatant was diluted and radioactive inositol phosphate (IP) species were isolated using anion-exchange chromatography. Radioactivity of the eluates was measured by β[−] counting on a liquid scintillation counter. Data were analyzed by nonlinear regression with GraphPad Prism 5.0.

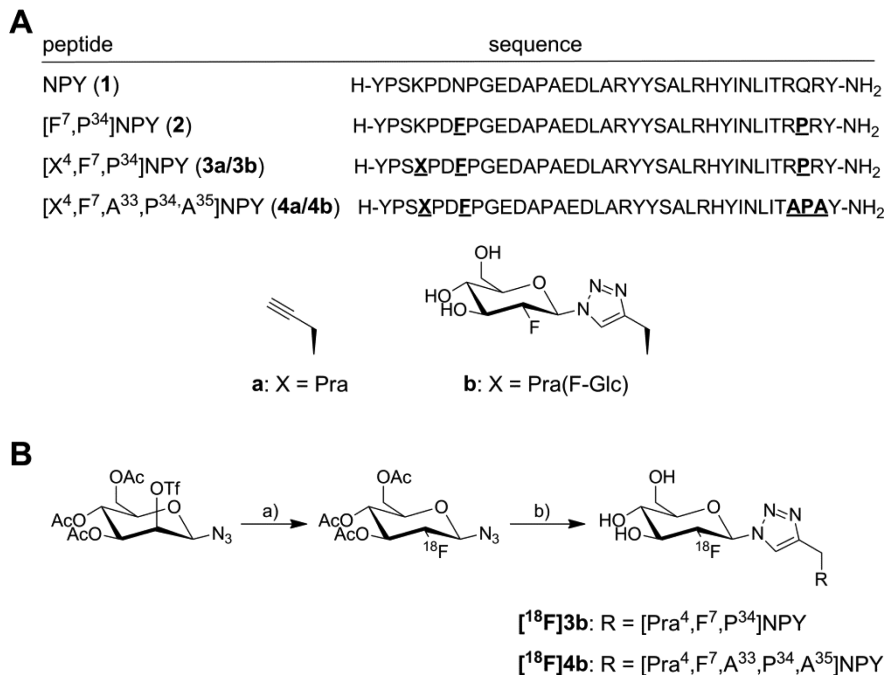


Figure 1. (A) Amino acid sequence of porcine NPY (**1**) and Y₁R-preferring NPY analogues (**2–4**): **3a/4a** = alkynylated precursor, **3b/4b** = nonradioactive surrogates. Respective amino acid replacements are indicated in bold and are underlined. (B) Radiosyntheses of [¹⁸F]3b and [¹⁸F]4b: (a) [¹⁸F]fluoride, K₂₂₂/K₂CO₃/KH₂PO₄, CH₃CN, 85 °C, 2.5 min; (b) 1. 60 mM NaOH, 60 °C, 5 min, 2. 1 M HCl, **3a** or **4a**, sodium ascorbate, CuSO₄, THPTA, 50 °C, 10 min.

¹²⁵I-PYY Displacement Assay. Bovine serum albumin fraction V (BSA) was purchased from PAA and Roth, respectively. Pefabloc SC was supplied by Fluka. [¹²⁵I]-hPYY, glass fiber filters Printed Filtermat B, Melt-on Scintillator Sheets MeltiLex A, and Sample Bags for MicroBeta were purchased from PerkinElmer. For competition binding assay, fresh stock solutions of [¹²⁵I]-hPYY were prepared (1 nM in 1% BSA/H₂O (w/v)). Peptide stock solutions were prepared by a 10-fold and 3.16-fold serial dilution in 1% BSA/H₂O (w/v). Cells were resuspended in assay medium, containing DMEM/Ham's F12, 50 μM of Pefabloc, and 1% BSA (w/v), and adjusted to a concentration of 6.25×10^5 cells/mL. Eighty microliters of cell suspension (5×10^4 cells) was seeded into 96-well plates and incubated with 10 μL of radioligand (final concentration: 100 pM) and 10 μL of increasing concentrations of cold peptide for 1 h at ambient temperature under continuous shaking. Competition binding was terminated by filtration through a glass fiber filter presoaked with 30 mL of 0.1% polyethylenimine (PEI) using a FilterMate Harvester (PerkinElmer). Filters were rapidly washed four times with ice-cold PBS and dried at 57 °C for 40 min in a Hybridization Oven/Shaker (Amersham Pharmacia Biotech). Dried filters were sealed with Melt-on Scintillator Sheets MeltiLex A on an electrical heating plate and shrink-wrapped in Sample Bags for MicroBeta. Radioactivity was measured in a MicroBeta² Plate Counter (2450 Microplate Counter, PerkinElmer) and analyzed by GraphPad Prism 5.03 software. IC₅₀ and pIC₅₀ values were calculated from sigmoidal concentration-response curves using nonlinear regression curve fit according to equation log(inhibitor) vs. response (three parameters).

Receptor Internalization Studies. Fluorescence microscopy studies were performed as previously described.²⁹ Briefly, to investigate peptide ligand induced receptor internalization, stably transfected HEK293 cells were seeded into μ-Slide 8-well chambered coverslips. After 1 h of starving in OptiMem

medium, containing Hoechst 33342 nuclei stain, cells were stimulated with 1.0 μM of peptide for 1 h at 37 °C. After washing receptor localization was visualized by live-cell fluorescence microscopy using AxioVision Rel. 4.6 software. For internalization studies with MCF-7 cells 100 nM of fluorescence-labeled peptide were used for stimulation. Blocking experiments were performed by costimulation with 100 nM of fluorescence-labeled peptide and 1 μM of either nonlabeled peptide **2** or BIBP3226 antagonist. After 1 h of stimulation, cells were treated once with a acidic wash solution (0.2 M glycine and 0.15 M NaCl in H₂O, pH 3.0) and twice with phosphate buffered saline and cultured in OptiMem for subsequent microscopy studies.

In Vivo Characterization. Tumor Model. All animal experiments were performed in compliance with the protocols approved by the local Animal Protection Authorities (Regierung Mittelfranken, Germany, No. 54-2532.1-22/10). Female athymic nude mice (nu/nu) were obtained from Harlan Winkelmann GmbH (Borchen, Germany) at 7–8 weeks of age and were kept under standard conditions (12 h light/dark) with food and water available *ad libitum*. Pellets containing 17β-estradiol (0.72 mg/pellet; release time, 60 days; Innovative Research of America, Sarasota, FL, USA) were placed subcutaneously in the interscapular region of the mice. MCF-7 cells were harvested and suspended in sterile PBS/Matrigel (1:1 v/v) at a concentration of 5×10^7 cells/mL, respectively. Viable cells (5×10^6) in PBS/Matrigel (100 μL) were injected subcutaneously into the back. Three weeks after inoculation (tumor weight, 50–180 mg), the mice (about 15–20 weeks old with about 40 g body weight) were used for biodistribution and small-animal PET studies.

Biodistribution Study. [¹⁸F]3b (1.5–2.5 MBq/mouse, *n* = 3–4 per time point) was intravenously injected into the MCF-7 xenografted mice via the tail vein. Mice were sacrificed by cervical dislocation 20, 60, and 120 min postinjection (p.i.).

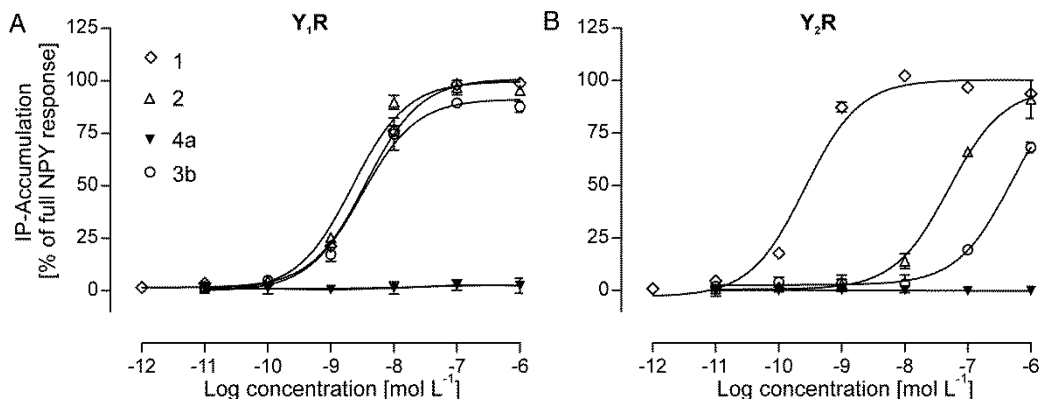


Figure 2. Relative inositol phosphate (IP) accumulation after 1 h stimulation with NPY (**1**) or Y₁R-preferring analogues. NPY (**1**) and [F⁷P³⁴]NPY (**2**) served as positive and the nonfunctional precursor [Pra⁴,F⁷,A³³,P³⁴,A³⁵]NPY (**4a**) as negative control. *In vitro* potencies at Y₁R (A) and Y₂R (B) were determined using stably transfected COS-7 cells. Data represent the total means \pm SEM of at least two independent experiments each performed as duplicates (Table 1). Receptor activation is expressed as percentage of full NPY response.

Tumors and other tissues (blood, lung, liver, kidneys, heart, spleen, muscle, brain, adrenal glands, thyroid, femur, pancreas, gall bladder, and duodenum) were removed and weighed. Radioactivity of the dissected tissues was determined using a γ -counter. Results were expressed as percentage of injected dose per gram of tissue (%ID/g), and tumor-to-organ ratios were calculated. Blocking experiments were carried out by intravenously coinjecting peptide **2** (250 μ g/mouse, $n = 4$) or BIBP3226 (1 mg/kg, $n = 3$) together with the radiotracer into randomly chosen mice. The mice were sacrificed by cervical dislocation 60 min p.i. Organs and tissues were removed, weighed, and counted as described above.

Small Animal PET. PET scans and image analysis were performed using a small animal PET rodent model scanner (Inveon, Siemens Medical Solutions). About 2–5 MBq of [¹⁸F]**3b** ($n = 14$) or [¹⁸F]**4b** ($n = 4$) were intravenously injected into each mouse under isoflurane anesthesia (3%). Animals were subjected to a 15 min scan starting from 45 min p.i.. Four animals injected with [¹⁸F]**3b** were scanned from 45 to 90 min p.i. For each small-animal PET scan, regions of interest (ROIs) were drawn over the tumor on decay-corrected whole-body images that were gained by 3D-OSEM iterative image reconstruction. The radioactivity concentration within the tumor was obtained from the mean value within the multiple ROIs and then converted to uptake values (%ID/g) by considering the injected dose. For receptor-blocking experiments, nude mice bearing MCF-7 tumors were scanned as described above (15 min scan, 45 min p.i.) after coinjection with [¹⁸F]**3b** (3–10 MBq) and **2** (125 or 250 μ g/animal, each $n = 2$).

RESULTS

Peptide Synthesis and Nonradioactive Fluoroglycosylation. On the basis of [F⁷P³⁴]NPY (**2**), which preferably binds to the breast cancer relevant Y₁R subtype,^{7,22} an alkyne-modified [F⁷P³⁴]NPY analogue (**3a**) was synthesized for subsequent fluoroglycosylation by click chemistry. Standard solid phase peptide synthesis using Fmoc/tBu strategy was applied. Alkyne functionalization was obtained by introduction of propargylglycine (Pra) at position 4, which has previously been described to be well-suited for diagnostic or therapeutic modifications.^{14,23,24} On the basis of **3a**, the corresponding nonbinding analogue (**4a**) containing an Arg³³/Arg³⁵ to Ala³³/Ala³⁵ substitution was synthesized and served as negative

control for the *in vivo* studies. The arginine residues, Arg³³ and Arg³⁵, have been described to be essential for YR binding and activation.^{31,32} Nonradioactive fluoroglycosylation of **3a** and **4a** resulted in corresponding F-Glc analogues **3b** and **4b**. These surrogates were used for the *in vitro* testing of YR activation potency and internalization pattern as well as reference compounds for radio-HPLC analysis. Peptide sequences and structures are summarized in Figure 1A. After automated peptide synthesis and manual introduction of Pra⁴, peptide precursors **3a** and **4a** were purified to final homogeneity of >95% confirmed by two independent RP-HPLC column systems. Peptide identity was verified by matrix-assisted laser desorption/ionization (MALDI) and electrospray ionization MS (ESI-MS). Analytical data are presented in Table S1. Nonradioactive fluoroglycosylation of **3a** and **4a** was successfully performed in solution under constant stirring and argon flow using 5 equiv of 2-deoxy-2-fluoro- β -D-glucosylazide²⁷ in a mixture of acetonitrile/phosphate buffer pH 8 (1:4 v/v) at 50 °C in the presence of CuSO₄ and ascorbic acid (1:3). The desired nonradioactive surrogates **3b** and **4b** were obtained in adequate yields of >85% for analytical scale and >65% for preparative scale within 30 min. Applying an optimized two-step gradient for semipreparative RP-HPLC final purities of >95% were obtained (Table S1) as demonstrated for surrogate **3b** in Figure S1.

In Vitro Characterization. Signal Transduction and Binding Assay. Receptor activation potencies of fluoroglycosylated surrogate **3b** and nonbinding precursor **4a** were investigated by a functional inositol phosphate accumulation assay using stably transfected COS-7 cells expressing one distinct YR subtype and the chimeric G $\alpha_{\Delta 6 q i 4 m y r}$ -protein³⁰ to switch from the endogenous inhibitory G α_i -protein pathway to the G α_q -protein pathway, which results in the intracellular generation of inositol trisphosphate. NPY (**1**) and [F⁷P³⁴]NPY (**2**) were included as respective controls. With respect to Y₁R, comparable EC₅₀ values for **1** and **2** of 3.6 and 2.2 nM, respectively, were determined. Surrogate **3b** (3.1 nM) displayed comparable potency to controls **1** and **2**. Activation efficacies and corresponding concentration-response curves are close to identical (Figure 2A). For the Y₂R, the potency values are different. As expected, for NPY (**1**) a subnanomolar EC₅₀ value of 0.3 nM was determined; [F⁷P³⁴]NPY (**2**) showed a 160-fold decreased potency (50.1 nM). The efficacy values for **1** (103 \pm 3%) and **2** (96 \pm 5%) are in the same range. For surrogate **3b**,

Table 1. *In Vitro* Potencies (EC_{50}) and Efficacies (E_{max}) as well as Binding Affinities (IC_{50}) of the Nonradioactive Fluoroglycosylated [$Pra^4(F\text{-Glc})F^7P^{34}]NPY$ (3b), the Corresponding Nonbinding Precursor (4a), and Control Peptides NPY (1) and [$F^7P^{34}]NPY$ (2); Additionally the Y_1R Antagonist BIBP3226 Was Tested

	YR activation ^a						Y ₁ R binding affinity			
	Y ₁ R			Y ₂ R			HEK_Y ₁ R		MCF-7	
	EC_{50} [nM] (pEC ₅₀ ± SEM) ^b	E_{max} [%] ^c	n	EC_{50} [nM] (pEC ₅₀ ± SEM) ^b	E_{max} [%] ^c	n	IC_{50} [nM] (pIC ₅₀ ± SEM) ^b	n	IC_{50} [nM] (pIC ₅₀ ± SEM) ^b	n
1	3.6 (8.44 ± 0.03)	99	30	0.3 (9.58 ± 0.05)	103	24	1.5 (8.82 ± 0.02)	9	1.3 (8.90 ± 0.08)	3
2	2.2 (8.66 ± 0.06)	100	5	50.1 (7.30 ± 0.11)	96	5	0.8 (9.10 ± 0.08)	3	0.9 (9.04 ± 0.20)	2
3b	3.1 (8.51 ± 0.10)	91	3	>1000 ^e	68	3	2.4 (8.63 ± 0.09)	2	2.8 (8.55 ± 0.17)	2
4a	ND ^d	ND	2	ND	ND	3	ND	2	ND	2
BIBP3226							6.7 (8.17 ± 0.11)	2	6.6 (8.18 ± 0.18)	2

^ahYR activation was investigated using stably transfected COS-7 cells. ^bValues represent the total mean of the EC_{50} / IC_{50} of all independent experiments of each peptide and its corresponding pEC₅₀/pIC₅₀ (±SEM) calculated with Prism 5.0 software. ^c E_{max} values ± SEM were obtained from concentration–response curves using the total mean of the highest concentration tested of all independent experiments normalized to NPY. ^dND: EC₅₀/IC₅₀ value could not be determined since no receptor activation/¹²⁵I-PYY displacement was observed up to 1 μM. ^eGreater than 1000: Estimated EC₅₀ value since no saturated receptor activation is reached up to 1 μM.

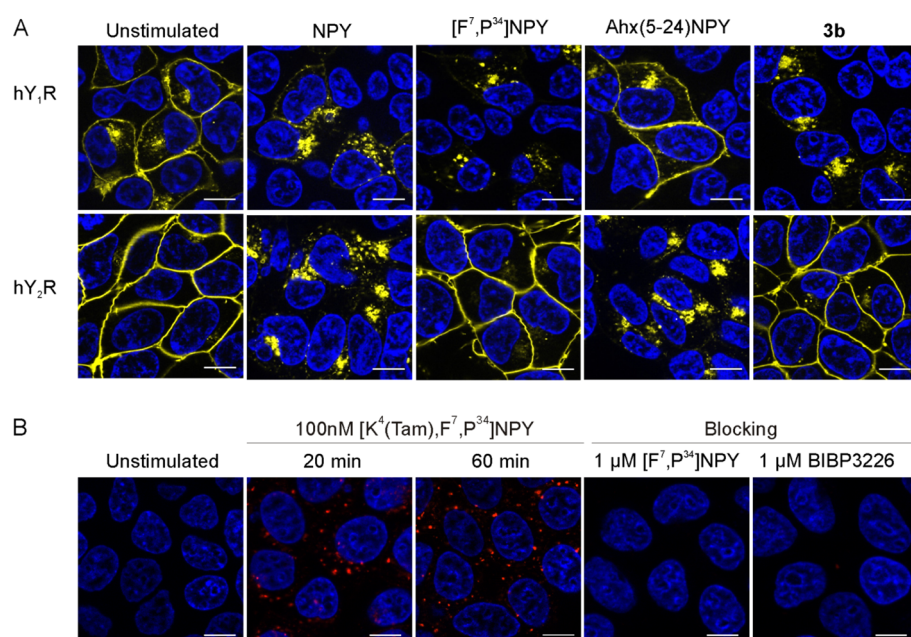


Figure 3. Live-cell fluorescence microscopy. (A) Receptor internalization was investigated after 1 h stimulation with 1 μM of peptide ligand by using stably transfected HEK293 cells that express either the Y_1R or Y_2R fused to the enhanced yellow fluorescent protein EYFP (yellow). Nuclei were stained with Hoechst 33342 (blue). Representative images of two independent experiments are shown. Scale bars represent 10 μm. NPY (1) served as positive control for both receptor subtypes, [$F^7P^{34}]NPY$ (2) as positive control for Y_1R , and Ahx(5–24)NPY as positive control for Y_2R . Compound 3b refers to the nonradioactive surrogate [$Pra^4(F\text{-Glc})F^7P^{34}]NPY$. (B) Receptor internalization was investigated for MCF-7 cells after 20 and 60 min stimulation with 100 nM 5(6)-carboxytetramethylrhodamine (Tam)-labeled peptide ligand. For blocking experiments, cells were costimulated with 1 μM of nonlabeled agonist 2 or BIBP3226 antagonist for 60 min. For all images a constant illumination time for the red fluorescence channel of 1 s was used.

the potency is further decreased >20-fold. The activation efficacy is decreased by 30% (68 ± 3%). Accordingly, the concentration–response curves of 2 and 3b are shifted to the higher nanomolar range, while for surrogate 3b no upper plateau is reached up to 1 μM (Figure 2B). The nonfunctional precursor 4a was found to be totally inactive at both YR subtypes (Table 1 and Figure 2).

Y_1R binding affinities were determined using ¹²⁵I-PYY displacement assay. To exclude potential differences between different cell lines, both the stably transfected HEK293 cells, expressing the Y_1R subtype (HEK_Y₁R), and MCF-7 cells, which were used for the generation of the breast cancer mouse model, were investigated. For native NPY an inherent low-nanomolar affinity was determined for both cell lines (IC_{50} : 1.5

and 1.3 nM) (Table 1). On the contrary, while the Y_1R -preferring analogue 2 and the fluoroglycosylated variant 3b displayed comparable low IC_{50} values as NPY at both HEK293_Y₁R and MCF-7 cells, no binding was observed for the nonbinding analogue 4a (Table 1). The small molecule antagonist BIBP3226 exhibited a slightly reduced but still low-nanomolar affinity (IC_{50} : 6.7 and 6.6 nM).

Receptor Internalization Studies. Ligand-induced receptor internalization was investigated by live-cell fluorescence microscopy using stably transfected HEK293 cells expressing either the Y_1R or the Y_2R , each C-terminally tagged with EYFP to evaluate the activity and the selectivity under similar conditions. Depending on the YR subtype the initial receptor localization differs slightly. The Y_1R can be found mainly on the

cell surface but to a lesser extent also intracellular. In contrast, the Y₂R is exclusively located on the cell surface (Figure 3A, unstimulated). However, after 1 h of stimulation with NPY (1) both YR subtypes are clearly internalized as indicated by the intracellular vesicular distribution of the fluorescence signals (Figure 3A, NPY). In accordance to the signal transduction data, internalization was only observed for the Y₁R but not for the Y₂R after stimulation with [F⁷,P³⁴]NPY (2) (Figure 3A, [F⁷,P³⁴]NPY). As an additional control, the Y₂R selective analogue Ahx(5–24)NPY³³ was investigated and displayed Y₂R selective internalization (Figure 3A, Ahx(5–24)NPY). Accordingly, surrogate **3b** shows the similar activity as **2** by clearly inducing Y₁R internalization, whereas the Y₂R remains on the cell surface. To *in vitro* characterize the Y₁R-mediated peptide internalization in MCF-7 cells, which were used for the generation of the breast cancer mouse model, a fluorescence-labeled variant of the Y₁R-preferring analogue **2** was used. Instead of the fluoroglycosyl-residue in position 4, this analogue carried a 5(6)-carboxytetramethylrhodamine (TAMRA, Tam) at the ε-NH₂ group of lysine 4. After stimulation of MCF-7 cells with (K⁴(Tam),F⁷,P³⁴]NPY for 20 and 60 min, the peptide was clearly internalized as indicated by intracellular red fluorescence spots (Figure 3B). Costimulation with a 10-fold excess of either **2** or BIBP3226 antagonist resulted in a significant reduction of the intracellular fluorescence signals (Figure 3B).

Radiochemistry. ^{[18]F}3b and ^{[18]F}4b were synthesized by ¹⁸F-fluoroglycosylation using 2-deoxy-2-[¹⁸F]fluoroglucosyl azide as described before²⁷ with slight modifications (Figure 1B). After deacetylation of the intermediate 3,4,6-tri-O-acetyl-2-deoxy-2-[¹⁸F]fluoroglucosyl azide, the pH of the reaction mixture was adjusted to pH 8 and the copper-catalyzed azide–alkyne cycloaddition (CuAAC) was performed with alkyne-bearing precursor peptides **3a** or **4a** in the presence of CuSO₄, sodium ascorbate, and THPTA. The presence of THPTA allowed us to reduce the amount of alkyne-bearing peptides to an optimal minimum of 40 nmol (0.1 mM). The radiochemical yield of the CuAAC was 70–80% after 10 min at 50 °C. ^{[18]F}3b and ^{[18]F}4b were obtained in overall radiochemical yields of 20–25% (nondecay corrected, referred to [¹⁸F]fluoride) in a total synthesis time of 75 min with specific activities of 40–70 GBq/μmol and high radiochemical purity (Figure S2).

In Vitro Characterization of ^{[18]F}3b. The logD_{7.4} value of ^{[18]F}3b was -0.8 ± 0.2 ($n = 3$), predicting adequate hydrophilicity for sufficient accumulation of the tracer in peripheral tumors together with suitable clearance properties through the kidneys. Incubation studies of the radiotracers in human plasma revealed high stability of ^{[18]F}3b and ^{[18]F}4b with >94% intact radiotracer at 37 °C after 60 min (Figure S2). Furthermore, specific binding of ^{[18]F}3b at Y₁R was investigated *in vitro* using MCF-7 tumor slices. The slices were incubated with ^{[18]F}3b, and subsequent autoradiography depicted high binding of glycopeptide ^{[18]F}3b in comparison with slices that were incubated in the presence of the nonradioactive competitor **3a** (1.25 μM) or BIP3226 (1 μM; Figure 4). The total binding of ^{[18]F}3b was reduced by 95% in the presence of **3a** and by 86% when BIP3226 was used as competitor, indicating high specific binding of ^{[18]F}3b to Y₁R expressed on MCF-7 tumors.

In Vivo Characterization of ^{[18]F}3b. The results of the biodistribution studies using MCF-7 tumor-bearing nude mice are presented in Figure 5 and Table S2. At the investigated time

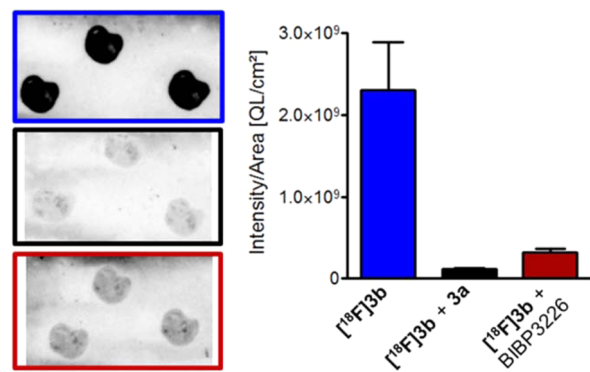


Figure 4. *In vitro* autoradiograms of MCF-7 tumor slices (three on each slide) incubated with ^{[18]F}3b alone (blue frame) and in the presence of **3a** (1.25 μM, black frame) or BIBP3226 (1 μM, red frame).

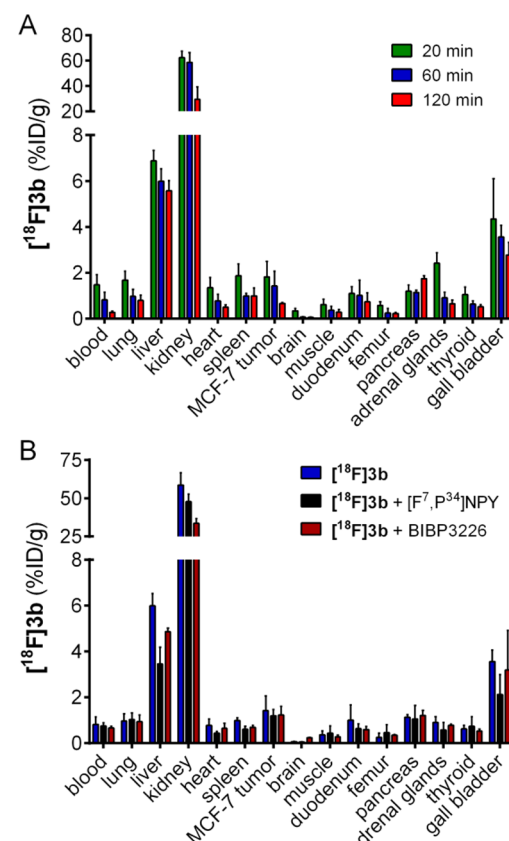


Figure 5. (A) Biodistribution of ^{[18]F}3b in MCF-7 tumor-bearing nude mice 20, 60, and 120 min p.i. and (B) under blocking conditions 60 min p.i. using **2** ([F⁷,P³⁴]NPY, 8 mg/kg) or BIBP3226 (1 mg/kg). Values are expressed as percentage injected dose per gram (%ID/g) of tissue (mean \pm SD, $n = 3$ –4).

points at 20, 60, and 120 min post injection (p.i.), ^{[18]F}3b displayed marked uptake in the kidneys (62–30%ID/g), moderate uptake and slow wash-out in liver and gall bladder (6.9–5.6%ID/g and 4.4–2.8%ID/g, respectively), and rapid clearance from the blood pool (1.5–0.3%ID/g). The uptake of ^{[18]F}3b in the MCF-7 tumor was 1.8%ID/g at 20 min p.i. and 0.7%ID/g at 120 min p.i., revealing tumor-to-blood ratios increasing from 1.2 to 2.4 and a tumor retention of $76 \pm 4\%$ ($n = 4$; 45–90 min p.i.) as determined from PET imaging data. However, animals that were injected with both ^{[18]F}3b and **2**

([F⁷,P³⁴]NPY, 8 mg/kg) or BIBP3226 (1 mg/kg) did not show any significant reduction in MCF-7 tumor uptake at 60 min p.i. (Figure 5B). The same result was obtained by small-animal PET experiments applying different doses of the blocking compound 2 (Figure 6A). Neither 125 µg (4 mg/kg) of 2 nor

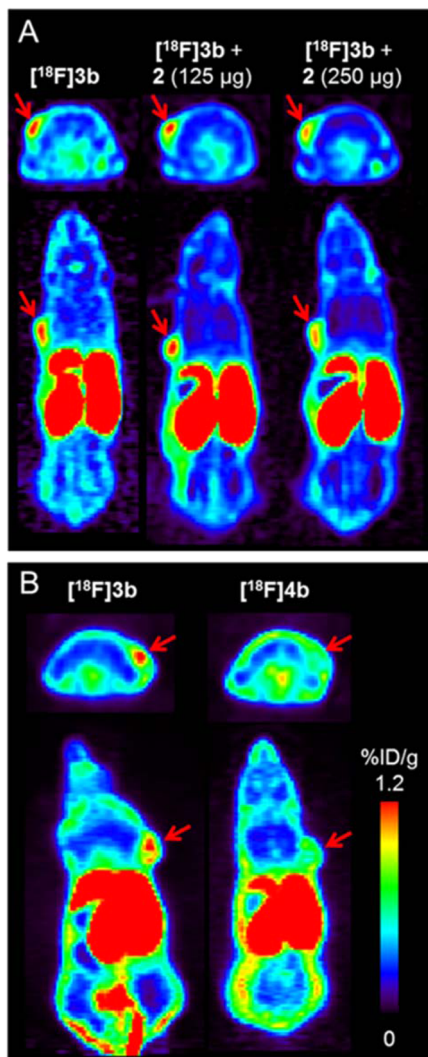


Figure 6. Representative transaxial (bottom) and coronal (top) μ PET images of MCF-7 tumor-bearing nude mice 45–60 min after administration of 2–5 MBq [¹⁸F]3b and under blocking conditions with 125 µg (4 mg/kg) or 250 µg (8 mg/kg) of 2 ([F⁷,P³⁴]NPY) (A), and μ PET images of animals injected with [¹⁸F]3b in comparison with the nonbinding peptide [¹⁸F]4b at 45–60 min p.i. (B). Red arrows indicate the MCF-7 tumor. The scale bar refers to both panels of the figure.

the doubled amount of 250 µg (8 mg/kg) led to a significant reduction of the tumor uptake in the time frame at 45–60 min postinjection ($1.04 \pm 0.17\%$ ID/g ($n = 14$) vs $1.04 \pm 0.18\%$ ID/g (4 mg/kg, $n = 2$) vs $0.92 \pm 0.12\%$ ID/g (8 mg/kg, $n = 2$); $P > 0.05$ (unpaired t test), see also Figure S4). To exclude that this observation is due to accelerated tracer degradation in the blood, we determined the stability of [¹⁸F]3b *in vivo* by HPLC analysis of blood samples taken at 10 min after injection of the tracer. The results showed two minor polar metabolites and a significant portion of 74% intact parent compound, clearly confirming an adequate stability of the glycopeptide *in vivo* (Figure S3).

Aiming at a more reliable definition of nonspecific binding of high-molecular-weight PET tracers, we conducted PET scans with the nonbinding NPY glycopeptide [¹⁸F]4b, and the results were compared to the same animal injected with [¹⁸F]3b (Figure 6B). The MCF-7 tumor was clearly visualized in the control animal injected with [¹⁸F]3b at 60 min p.i., whereas only negligible tumor uptake was determined in animals injected with the low-affinity peptide [¹⁸F]4b as a measure of nonspecific binding ($1.04 \pm 0.17\%$ ID/g ($n = 14$) vs $0.60 \pm 0.10\%$ ID/g ($n = 4$); $P < 0.01$ (unpaired t test), see also Figure S4). Comparing the PET data of both experiments, we observed a difference in tracer uptake of 40%, using at least four independent animals for each experimental group. These results successfully confirmed the specificity of glycopeptide [¹⁸F]3b for imaging Y₁R positive tumors *in vivo* by PET.

DISCUSSION

This article reports the first ¹⁸F-labeled high-molecular-weight NPY glycopeptide tracer for PET imaging of Y₁R expression in a preclinical animal model of breast cancer. Although recently an ¹⁸F-labeled small-molecule ligand for imaging Y₁R in the brain has been published, this tracer is a lipophilic nonpeptide ligand, which has not been tested for uptake in peripheral tumors.²⁵

The design of glycoconjugate 3b as potential PET tracer was based on previous structure–activity relationship studies on NPY revealing that modifications of the lysine residue in position 4 are well tolerated in terms of Y₁R/Y₂R binding.³¹ Subsequently, lysine 4 has been successfully established as suitable position for the introduction of diverse cargos in the Y₁R-preferring analogue [F⁷,P³⁴]NPY such as fluorescence dyes, chelators for radiolabeling, or carbaboranes for boron neutron capture therapy.^{23,24} These modified analogues were shown to maintain a low-nanomolar Y₁R binding affinity and activation potency.

The various commonly applied classical ¹⁸F-labeling methods for peptides, such as ¹⁸F-acylation with [¹⁸F]SFB or others,³⁴ have the disadvantage that they are not regiospecific, not highly chemoselective, and increase the lipophilicity of the resulting radiopeptide. In the present work, we have successfully adapted our click chemistry based ¹⁸F-fluoroglycosylation method to achieve the successful radiosynthesis of the ¹⁸F-labeled NPY glycopeptide conjugate [¹⁸F]3b. By using the ¹⁸F-fluoroglycosylation method, we aimed at the improvement of hydrophilicity of this large molecule to shift its biodistribution toward reduced liver uptake and increased renal clearance, and simultaneously taking advantage of the superior regiospecificity of the click chemistry labeling reaction that allowed us to introduce the ¹⁸F-fluoroglycosyl moiety in position 4 of the amino acid sequence in a very reliable manner. As compared to previous results for the position 4 modified ¹¹¹In-labeled DOTA-NPY analogue (kidney: 77%ID/g at 2 h p.i.),²³ the glycopeptide conjugate [¹⁸F]3b displayed significantly increased renal clearance properties (30%ID/g; Table S2), providing evidence for our hypothesis that glycosylated radiopeptides demonstrate favorable kinetics *in vivo*.

In the present study, the MCF-7 breast cancer tumor model has been used as preclinical animal model. It is reported that MCF-7 xenografts show limited vascularization *in vivo*.³⁵ However, one major advantage of the MCF-7 cells is their Y₁R surface expression level of $1–3 \times 10^5$ sites/cell³⁶ that appears to be in a similar range as for other tumor-relevant GPCRs, such as the gastrin-releasing peptide receptor (GRPR)

on PC-3 human prostate cancer cells^{37,38} or the somatostatin receptor-2 (sst2) on AR24J rat pancreatic cancer cells (1.5×10^5 sites/cell).³⁴ However, the exact number of Y₁R sites/cell on MCF-7 cells *in vivo* might differ from the *in vitro* data because the more complex *in vivo* microenvironment might have an influence on the Y₁R expression level.^{37,38} Nonetheless, on the basis of the strong and displaceable binding of the glycopeptide [¹⁸F]3b demonstrated by *in vitro* autoradiography with MCF-7 tumor slices, we assume a sufficient Y₁R surface expression level in the MCF-7 tumor.

The *in vitro* characterization of the cold fluoroglycosylated analogue 3b demonstrated a high Y₁R binding affinity, activity, and Y₁R-mediated internalization. Using a corresponding fluorescence-labeled analogue, a fast and effective intracellular accumulation in MCF-7 cells could be demonstrated, that can be blocked by costimulation with 2 or BIBP3226. Together with the strong and competitive binding of [¹⁸F]3b to MCF-7 xenograft tumor slices, these results suggested that [¹⁸F]3b can be efficiently taken up *in vivo* by MCF-7 tumors. However, the specific *in vivo* binding of the high-molecular-weight tracer [¹⁸F]3b was difficult to determine both in competition PET and biodistribution studies (Figures 5B and 6A). By applying either the peptide precursor [F⁷,P³⁴]NPY (2) or the low-molecular-weight Y₁R antagonist BIBP3226, a significant competition could not be achieved. This observation could be explained by considering different *in vivo* kinetic and metabolic properties of the radiotracer [¹⁸F]3b and the blocking compounds 2 and BIBP3226. For molecules of highly different sizes, different *in vivo* tumor uptake and clearance properties have been described.³⁹ It has been suggested that shorter peptides or small molecules are transported more quickly through the lymphatic system as it has been described for short peptidic and small molecule neuropeptidergic receptor radioligands.^{28,40} This effect is due to the fact that tumors have leaky vessels and that clearance of large molecules proceeds slowly through the lymphatic system. Therefore, the competitive effect of coinjection of a small molecule Y₁R antagonist on binding of [¹⁸F]3b *in vivo* might be hindered owing to different tumor penetration kinetics and overall clearance properties. We suppose that the short antagonist BIBP3226 with a molecular weight of 500 Da is able to rapidly penetrate into the tumor followed by a fast release and body clearance. In contrast, the larger [¹⁸F]3b peptide tracer with a 10-fold increased molecular weight of 4 kDa is supposed to enter the tumor more slowly, resulting in a time-shifted arrival of both molecules at the receptor sites within the tumor. Consequently, [¹⁸F]3b is able to bind and internalize into the tumor cells without a competitive effect by BIBP3226.

For the competitive effect of cold [Phe⁷,Pro³⁴]NPY (2) on binding of [¹⁸F]3b *in vivo*, the kinetic issue is of less relevance since both molecules are of comparable size. Here, we assume that the *in vivo* competition might be hindered owing to a lower metabolic stability of [Phe⁷,Pro³⁴]NPY (2) compared to the fluoroglycosylated radiotracer [¹⁸F]3b because glycosylation has been described to enhance the peptide stability through direct spatial shielding of protease cleavage sites.^{41,42} Native NPY has been shown to be rapidly degraded by N-terminal proteolytic cleavage, resulting in NPY (3–36), which displays only weak Y₁R affinity.⁴³ Accordingly, the coinjected cold [Phe⁷,Pro³⁴]NPY (2) is supposed to be N-terminally attacked by proteolytic enzymes and loses its Y₁R affinity, while the glycosyl-residue at position 4 protects [¹⁸F]3b from degradation. Thus, both peptides might penetrate the tumor in a

comparable manner, but only [¹⁸F]3b is able to bind Y₁R followed by internalization. With respect to the potential *in vivo* kinetic and metabolic drawback of the large NPY-based radiotracer, stabilized reduced-size Y₁R variants are under current investigation.

Very recently, a clinical study for the diagnostic imaging of breast tumors by PET using 16α -[¹⁸F]fluoro-17 β -estradiol ([¹⁸F]FES) as a tracer for estrogen receptors has been reported.⁴⁴ This work reports on the importance of factors influencing the imaging results through affecting the fraction of free receptors and tumor [¹⁸F]FES uptake, such as menopausal status and concomitant therapies. Since additional studies are clearly needed that address these issues, we assume that alternative PET tracers such as [¹⁸F]3b or derivatives thereof could add value to improve our knowledge on tracer-specific PET imaging of breast carcinoma.

Benefits of Y₁R imaging in addition to estrogen receptor (ER) imaging include the exclusive Y₁R expression on tumor cells, not in healthy breast tissue, and the tremendous high incidence on metastatic lesions.⁴⁵ In contrast, the ER is described to be expressed in both normal breast tissue and on tumor cells.⁴⁶ Furthermore, although the majority of breast cancer tumors are ER-positive, a number of very aggressive so-called triple-negative forms occur, which have the worst prognoses among all subtypes.⁴⁷ In this case, Y₁R imaging might be suggested as a supporting strategy.

CONCLUSION

Taken together, the ¹⁸F-labeled NPY glycopeptide [¹⁸F]3b demonstrated high activity and excellent subtype selectivity for Y₁R over Y₂R *in vitro*. The PET imaging experiments with [¹⁸F]3b revealed partial Y₁R-specific uptake in MCF-7 tumors *in vivo* together with decreased kidney uptake compared to DOTA-derivatives of this peptide. We consider the glycopeptide [¹⁸F]3b to be the lead peptide for the design of improved radiopeptides with shorter amino acid sequences that would further facilitate PET imaging studies of Y₁R expression in breast tumors.

ASSOCIATED CONTENT

Supporting Information

General information on materials and methods, solid phase peptide synthesis, determination of distribution coefficient at pH 7.4 (logD_{7.4}), determination of tracer stability in human serum, *in vitro* autoradiography (Y₁R detection in MCF-7 tumor slices), and stability in mouse blood *ex vivo*; analytical data of 3a, 3b, 4a, and 4b; Table S1. Biodistribution of [¹⁸F]3b; Table S2. Analytical data of fluoroglycosylated [Pra⁴(F-Glc),F⁷,P³⁴]NPY analogue 3b; Figure S1. Purity, identity, and stability of [¹⁸F]3b and [¹⁸F]4b; Figure S2. *In vivo* stability of [¹⁸F]3b; Figure S3. Tumor uptake values as determined by PET imaging; Figure S4. This material is available free of charge via the Internet at <http://pubs.acs.org>.

AUTHOR INFORMATION

Corresponding Author

*Molecular Imaging and Radiochemistry, Nuclear Medicine Clinic, Friedrich-Alexander University, Schwabachanlage 6, D-91054 Erlangen, Germany. Tel: +49-9131-8544440. Fax: +49-9131-8534440. E-mail: olaf.prante@uk-erlangen.de.

Notes

The authors declare no competing financial interest.

ACKNOWLEDGMENTS

The authors thank Bianca Weigel and Manuel Geisthoff (FAU) and Kristin Löbner, Regina Reppich-Sacher, and Christina Dammann (Univ. Leipzig) for excellent technical support. PET Net GmbH (Erlangen-Tennenlohe) is acknowledged for delivering n.c.a. F-18. This work was supported by the Deutsche Forschungsgemeinschaft (DFG, grants MA 4295/1-2, PR 677/5-1, BE 1264/9-2 (FOR630)). We further express our thanks to the DFG Research Training Group *Medicinal Chemistry of Selective GPCR Ligands* (GRK 1910) and the Graduate School *Leipzig School of Natural Sciences: Building with Molecules and Nano-objects* (BuildMoNa). The project was partially funded by the European Union and the Free State of Saxony.

REFERENCES

- (1) Heng, B. C.; Aubel, D.; Fussenegger, M. An overview of the diverse roles of G-protein coupled receptors (GPCRs) in the pathophysiology of various human diseases. *Biotechnol. Adv.* **2013**, *31*, 1676–1694.
- (2) Rosenbaum, D. M.; Rasmussen, S. G.; Kobilka, B. K. The structure and function of G-protein-coupled receptors. *Nature* **2009**, *459*, 356–363.
- (3) Reubi, J. C.; Macke, H. R.; Krenning, E. P. Candidates for peptide receptor radiotherapy today and in the future. *J. Nucl. Med.* **2005**, *46* (Suppl 1), 67S–75S.
- (4) Reubi, J. C. Peptide receptors as molecular targets for cancer diagnosis and therapy. *Endocr. Rev.* **2003**, *24*, 389–427.
- (5) Langer, M.; Beck-Sickinger, A. G. Peptides as carrier for tumor diagnosis and treatment. *Curr. Med. Chem. Anticancer Agents* **2001**, *1*, 71–93.
- (6) Ahrens, V. M.; Bellmann-Sickert, K.; Beck-Sickinger, A. G. Peptides and peptide conjugates: therapeutics on the upward path. *Future Med. Chem.* **2012**, *4*, 1567–1586.
- (7) Reubi, J. C.; Gugger, M.; Waser, B.; Schaer, J. C. Y(1)-mediated effect of neuropeptide Y in cancer: breast carcinomas as targets. *Cancer Res.* **2001**, *61*, 4636–4641.
- (8) Reubi, J. C.; Gugger, M.; Waser, B. Co-expressed peptide receptors in breast cancer as a molecular basis for in vivo multireceptor tumour targeting. *Eur. J. Nucl. Med. Mol. Imaging* **2002**, *29*, 855–862.
- (9) Korner, M.; Reubi, J. C. NPY receptors in human cancer: a review of current knowledge. *Peptides* **2007**, *28*, 419–425.
- (10) Michel, M. C.; Beck-Sickinger, A.; Cox, H.; Doods, H. N.; Herzog, H.; Larhammar, D.; Quirion, R.; Schwartz, T.; Westfall, T. XVI. International Union of Pharmacology recommendations for the nomenclature of neuropeptide Y, peptide YY, and pancreatic polypeptide receptors. *Pharmacol. Rev.* **1998**, *50*, 143–150.
- (11) Herzog, H.; Hort, Y. J.; Ball, H. J.; Hayes, G.; Shine, J.; Selbie, L. A. Cloned human neuropeptide Y receptor couples to two different second messenger systems. *Proc. Natl. Acad. Sci. U.S.A.* **1992**, *89*, 5794–5798.
- (12) Bohme, I.; Stichel, J.; Walther, C.; Morl, K.; Beck-Sickinger, A. G. Agonist induced receptor internalization of neuropeptide Y receptor subtypes depends on third intracellular loop and C-terminus. *Cell. Signalling* **2008**, *20*, 1740–1749.
- (13) Schiøth, H. B.; Fredriksson, R. The GRAFS classification system of G-protein coupled receptors in comparative perspective. *Gen. Comp. Endocrinol.* **2005**, *142*, 94–101.
- (14) Khan, I. U.; Zwanziger, D.; Bohme, I.; Javed, M.; Naseer, H.; Hyder, S. W.; Beck-Sickinger, A. G. Breast-cancer diagnosis by neuropeptide Y analogues: from synthesis to clinical application. *Angew. Chem., Int. Ed.* **2010**, *49*, 1155–1158.
- (15) Tatemoto, K.; Carlquist, M.; Mutt, V. Neuropeptide Y—a novel brain peptide with structural similarities to peptide YY and pancreatic polypeptide. *Nature* **1982**, *296*, 659–660.
- (16) Larhammar, D. Evolution of neuropeptide Y, peptide YY and pancreatic polypeptide. *Regul. Pept.* **1996**, *62*, 1–11.
- (17) Lindner, D.; Stichel, J.; Beck-Sickinger, A. G. Molecular recognition of the NPY hormone family by their receptors. *Nutrition* **2008**, *24*, 907–917.
- (18) Lundell, I.; Blomqvist, A. G.; Berglund, M. M.; Schober, D. A.; Johnson, D.; Statnick, M. A.; Gadski, R. A.; Gehlert, D. R.; Larhammar, D. Cloning of a human receptor of the NPY receptor family with high affinity for pancreatic polypeptide and peptide YY. *J. Biol. Chem.* **1995**, *270*, 29123–29128.
- (19) Cabrele, C.; Beck-Sickinger, A. G. Molecular characterization of the ligand-receptor interaction of the neuropeptide Y family. *J. Pept. Sci.* **2000**, *6*, 97–122.
- (20) Babilon, S.; Morl, K.; Beck-Sickinger, A. G. Towards improved receptor targeting: anterograde transport, internalization and post-endocytic trafficking of neuropeptide Y receptors. *Biol. Chem.* **2013**, *394*, 921–936.
- (21) Fuhldendorff, J.; Gether, U.; Aakerlund, L.; Langeland-Johansen, N.; Thøgersen, H.; Melberg, S. G.; Olsen, U. B.; Thastrup, O.; Schwartz, T. W. [Leu³¹, Pro³⁴]neuropeptide Y: a specific Y1 receptor agonist. *Proc. Natl. Acad. Sci. U.S.A.* **1990**, *87*, 182–186.
- (22) Soll, R. M.; Dinger, M. C.; Lundell, I.; Larhammar, D.; Beck-Sickinger, A. G. Novel analogues of neuropeptide Y with a preference for the Y1-receptor. *Eur. J. Biochem.* **2001**, *268*, 2828–2837.
- (23) Zwanziger, D.; Khan, I. U.; Neundorf, I.; Sieger, S.; Lehmann, L.; Fribe, M.; Dinkelborg, L.; Beck-Sickinger, A. G. Novel chemically modified analogues of neuropeptide Y for tumor targeting. *Bioconjugate Chem.* **2008**, *19*, 1430–1438.
- (24) Ahrens, V. M.; Frank, R.; Stadlbauer, S.; Beck-Sickinger, A. G.; Hey-Hawkins, E. Incorporation of ortho-carboranyl-N^e-modified L-lysine into neuropeptide Y receptor Y1- and Y2-selective analogues. *J. Med. Chem.* **2011**, *54*, 2368–2377.
- (25) Hostetler, E. D.; Sanabria-Bohorquez, S.; Fan, H.; Zeng, Z.; Gantert, L.; Williams, M.; Miller, P.; O’Malley, S.; Kameda, M.; Ando, M.; Sato, N.; Ozaki, S.; Tokita, S.; Ohta, H.; Williams, D.; Sur, C.; Cook, J. J.; Burns, H. D.; Hargreaves, R. Synthesis, characterization, and monkey positron emission tomography (PET) studies of [¹⁸F]Y1-973, a PET tracer for the neuropeptide Y Y1 receptor. *NeuroImage* **2011**, *54*, 2635–2642.
- (26) Maschauer, S.; Prante, O. A series of 2-O-trifluoromethylsulfonyl-D-mannopyranosides as precursors for concomitant ¹⁸F-labeling and glycosylation by click chemistry. *Carbohydr. Res.* **2009**, *344*, 753–761.
- (27) Maschauer, S.; Einsiedel, J.; Haubner, R.; Hocke, C.; Ocker, M.; Hübner, H.; Kuwert, T.; Gmeiner, P.; Prante, O. Labeling and glycosylation of peptides using click chemistry: a general approach to ¹⁸F-glycopeptides as effective imaging probes for positron emission tomography. *Angew. Chem., Int. Ed.* **2010**, *49*, 976–979.
- (28) Maschauer, S.; Haubner, R.; Kuwert, T.; Prante, O. ¹⁸F-glyco-RGD peptides for PET imaging of integrin expression: efficient radiosynthesis by click chemistry and modulation of biodistribution by glycosylation. *Mol. Pharmaceutics* **2014**, *11*, 505–515.
- (29) Hofmann, S.; Frank, R.; Hey-Hawkins, E.; Beck-Sickinger, A. G.; Schmidt, P. Manipulating Y receptor subtype activation of short neuropeptide Y analogs by introducing carbaboranes. *Neuropeptides* **2013**, *47*, 59–66.
- (30) Kostenis, E. Is Galphai6 the optimal tool for fishing ligands of orphan G-protein-coupled receptors? *Trends Pharmacol. Sci.* **2001**, *22*, 560–564.
- (31) Beck-Sickinger, A. G.; Wieland, H. A.; Wittneben, H.; Willim, K. D.; Rudolf, K.; Jung, G. Complete L-alanine scan of neuropeptide Y reveals ligands binding to Y1 and Y2 receptors with distinguished conformations. *Eur. J. Biochem.* **1994**, *225*, 947–958.
- (32) Merten, N.; Lindner, D.; Rabe, N.; Rompler, H.; Morl, K.; Schoneberg, T.; Beck-Sickinger, A. G. Receptor subtype-specific docking of Asp6.59 with C-terminal arginine residues in Y receptor ligands. *J. Biol. Chem.* **2007**, *282*, 7543–7551.
- (33) Beck, A.; Jung, G.; Gaida, W.; Koppen, H.; Lang, R.; Schnorrenberg, G. Highly potent and small neuropeptide Y agonist obtained by linking NPY 1–4 via spacer to alpha-helical NPY 25–36. *FEBS Lett.* **1989**, *244*, 119–122.

- (34) Schottelius, M.; Wester, H. J. Molecular imaging targeting peptide receptors. *Methods* **2009**, *48*, 161–177.
- (35) Bzyl, J.; Lederle, W.; Rix, A.; Grouls, C.; Tardy, I.; Pochon, S.; Siepmann, M.; Penzkofer, T.; Schneider, M.; Kiessling, F.; Palmowski, M. Molecular and functional ultrasound imaging in differently aggressive breast cancer xenografts using two novel ultrasound contrast agents (BR55 and BR38). *Eur. Radiol.* **2011**, *21*, 1988–1995.
- (36) Keller, M.; Pop, N.; Hutzler, C.; Beck-Sickinger, A. G.; Bernhardt, G.; Buschauer, A. Guanidine-acylguanidine bioisosteric approach in the design of radioligands: synthesis of a tritium-labeled N-G-propionylargininamide ([H-3]-UR-MK114) as a highly potent and selective neuropeptide Y Y-1 receptor antagonist. *J. Med. Chem.* **2008**, *51*, 8168–8172.
- (37) Reile, H.; Armatis, P. E.; Schally, A. V. Characterization of high-affinity receptors for bombesin/gastrin releasing peptide on the human prostate-cancer cell-lines Pc-3 and Du-145 - internalization of receptor-bound (125)I-(Tyr(4)) bombesin by tumor-cells. *Prostate* **1994**, *25*, 29–38.
- (38) Sancho, V.; Di Florio, A.; Moody, T. W.; Jensen, R. T. Bombesin receptor-mediated imaging and cytotoxicity: review and current status. *Curr. Drug Delivery* **2011**, *8*, 79–134.
- (39) Wester, H. J.; Kessler, H. Molecular targeting with peptides or peptide-polymer conjugates: just a question of size? *J. Nucl. Med.* **2005**, *46*, 1940–1945.
- (40) Lang, C.; Maschauer, S.; Hübner, H.; Gmeiner, P.; Prante, O. Synthesis and evaluation of a ¹⁸F-labeled diarylpyrazole glycoconjugate for the imaging of NTS1-positive tumors. *J. Med. Chem.* **2013**, *56*, 9361–9365.
- (41) Sola, R. J.; Griebbenow, K. Effects of glycosylation on the stability of protein pharmaceuticals. *J. Pharm. Sci.* **2009**, *98*, 1223–1245.
- (42) Powell, M. F.; Stewart, T.; Otvos, L.; Urge, L.; Gaeta, F. C. A.; Sette, A.; Arrhenius, T.; Thomson, D.; Soda, K.; Colon, S. M. Peptide stability in drug development 0.2. effect of single amino-acid substitution and glycosylation on peptide reactivity in human serum. *Pharm. Res.* **1993**, *10*, 1268–1273.
- (43) Abid, K.; Rochat, B.; Lassahn, P. G.; Stocklin, R.; Michalet, S.; Brakch, N.; Aubert, J. F.; Vatansever, B.; Tella, P.; De Meester, I.; Grouzmann, E. Kinetic study of neuropeptide Y (NPY) proteolysis in blood and identification of NPY3–35 a new peptide generated by plasma kallikrein. *J. Biol. Chem.* **2009**, *284*, 24715–24724.
- (44) van Kruchten, M.; de Vries, E. G.; Brown, M.; de Vries, E. F.; Glaudemans, A. W.; Dierckx, R. A.; Schroder, C. P.; Hospers, G. A. PET imaging of oestrogen receptors in patients with breast cancer. *Lancet Oncol.* **2013**, *14*, e465–475.
- (45) Reubi, J. C.; Gugger, M.; Waser, B.; Schaer, J. C. Y-1-mediated effect of neuropeptide Y in cancer: Breast carcinomas as targets. *Cancer Res.* **2001**, *61*, 4636–4641.
- (46) De Abreu, F. B.; Schwartz, G. N.; Wells, W. A.; Tsongalis, G. J. Personalized therapy for breast cancer. *Clin. Genet.* **2014**, *86*, 62–67.
- (47) Glück, S. nab-Paclitaxel for the treatment of aggressive metastatic breast cancer. *Clin. Breast Cancer* **2014**, *14*, 221–227.